BELLCOMM, INC.
955 L'ENFANT PLAZA NORTH, S.W., WASHINGTON, D.C. 20024

COVER SHEET FOR TECHNICAL MEMORANDUM

TITLE- Digital Filtering for Optimization of Signals Submerged in Noise

TM-69-1033-2

DATE- October 7, 1969

FILING CASE NO(S)- 103-6

AUTHOR(S)- S. Y. Lee

FILING SUBJECT(S) (ASSIGNED BY AUTHOR(S))- Optics
Lunar Orbiter III Photographs
Digital Noise Filters
Optical Data Processing
Digital Optical Compensation

ABSTRACT

Photographic noise reduces the amount of image information that can be recorded. Using the two-dimensional Wiener-Hopf equation we derive optimum linear filters for performing a spatial filtering operation on inputs, where the input consists of signal plus white additive noise which have been recorded in a digital array as intensity values. As an illustrative example, four spatial correction filters were constructed from the modulation transfer function of Lunar Orbiter III. These filters have been used on a representative picture taken by Lunar Orbiter III.

SEE REVERSE SIDE FOR DISTRIBUTION LIST

BELLCOMM, INC.
955 L'ENFANT PLAZA NORTH, S.W. WASHINGTON, D.C. 20024

SUBJECT: Digital Filtering for Optimization of Signals Submerged in Noise - Case 103-6

DATE: October 7, 1969

FROM: S. Y. Lee

TM-69-1033-2

TECHNICAL MEMORANDUM

I. INTRODUCTION

Photographic noise reduces the amount of image information that can be recorded. This memorandum is concerned with the problem of deriving an optimum linear filter for performing a spatial filtering operation on inputs, where the input consists of signal plus white noise, which have been recorded in a digital array as intensity values. This problem essentially boils down to a two-dimensional generalization of the frequency-domain filtering of time series. It is well known from network theory that the one-dimensional Wiener-Hopf equation for optimum linear filters minimizes the mean-square error between input and the desired output, where the input and the desired output are in the form of distributions. Elias, Grey and Robinson show that the one-dimensional Wiener-Hopf equation can be generalized to the multidimensional cases. Therefore by using the two-dimensional Wiener-Hopf equation and assuming the desired output is a circular disc with uniform intensity,* optimum linear filters are derived for a given quantity indicative of signal to noise ratio.

II. THE TWO-DIMENSIONAL WIENER-HOPF EQUATION

Consider $I_m(x,y)$, $I_s(x,y)$ and $I_n(x,y)$ be the intensity distributions of the message, its signal and noise components respectively, and let $\phi_{m,m}(x,y)$, $\phi_{s,s}(x,y)$ and $\phi_{n,n}(x,y)$ be their autocorrelation functions. The cross-correlation function between signal and message can then be denoted by $\phi_{s,m}(x,y)$. When these functions are defined, the two-dimensional Wiener-Hopf equation is expressed as

---

*Resolution of a minimal disc was chosen in order to detect objects which can be approximated by a composite of discs of minimal size and larger. This is a two-dimensional analog to the ideal detection of a pulse for the one-dimensional case.

$$\phi_{s,m}(x,y) = \int_{-\infty}^{\infty}\int_{-\infty}^{\infty} h_{opt}(x',y')\phi_{m,m}(x-x',y-y')dx'dy' \qquad (1)$$

where $h_{opt}(x,y)$ is the unit-impulse response of the optimum linear system. Noting that the right-hand member of (1) is the convolution of the optimum unit impulse response and the input autocorrelation, by taking the Fourier transforms of both sides of (1) we obtain

$$\Phi_{s,m}(\omega_x,\omega_y) = H_{opt}(\omega_x,\omega_y)\Phi_{m,m}(\omega_x,\omega_y) \qquad (2)$$

or

$$H_{opt}(\omega_x,\omega_y) = \frac{\Phi_{s,m}(\omega_x,\omega_y)}{\Phi_{m,m}(\omega_x,\omega_y)} \qquad (3)$$

where $H_{opt}(\omega_x,\omega_y)$ is the system transfer function of the optimum linear filter, and $\Phi_{s,m}(\omega_x,\omega_y)$ and $\Phi_{m,m}(\omega_x,\omega_y)$ are the energy spectrums associated with $\phi_{s,m}(x,y)$ and $\phi_{m,m}(x,y)$ respectively. The energy spectrum is defined as

$$\Phi(\omega_x,\omega_y) = \int_{-\infty}^{\infty}\int_{-\infty}^{\infty} \phi(x,y)e^{-2\pi j(\omega_x x+\omega_y y)}dxdy \qquad (4)$$

If the signal and the noise are uncorrelated, equation (3) becomes

$$H_{opt}(\omega_x,\omega_y) = \frac{\Phi_{s,s}(\omega_x,\omega_y)}{\Phi_{m,m}(\omega_x,\omega_y)} \qquad (5)$$

III. NOISE FILTERING BY OPTIMAL LINEAR FILTERS

Assume that the object located in the center of the field is circular with radius r_0 as shown in Figure 1(a). On the background of this field there is a noise pattern which we shall assume is white additive in character. The object is to design linear filters so as to optimize the signal to noise ratio in the mean-square error sense.

By assuming the intensity of this circular object is uniform, the intensity distribution can be expressed in polar coordinates

$$I(r) = \begin{cases} I_0 \text{ for } 0 \leq r \leq r_0 \\ \\ 0 \quad \text{otherwise} \end{cases} \tag{6}$$

where I_0 is in terms of intensity per length square. To obtain the system transfer function of the optimum linear filter for this message we first have to find the autocorrelation function of the signal and its energy spectrums, then rewriting (5) for the case of white additive noise

$$H_{opt}(\omega_x,\omega_y) = \frac{\Phi_{s,s}(\omega_x,\omega_y)}{\Phi_{s,s}(\omega_x,\omega_y) + \Phi_{n,n}(\omega_x,\omega_y)} \tag{7}$$

The autocorrelation function of the signal intensity distribution (6) can be readily calculated using the following expression

$$\phi'_{s,s}(\xi) = \begin{cases} \int_0^{\infty} \int_0^{2\pi} I(r)\ I(R) r\,dr\,d\theta \text{ for } 0 \leq \xi \leq 2r_0 \text{ where} \\ R^2 = r^2 + \xi^2 - 2r\xi \cos\theta \\ \\ 0 \quad \text{otherwise} \end{cases} \tag{8}$$

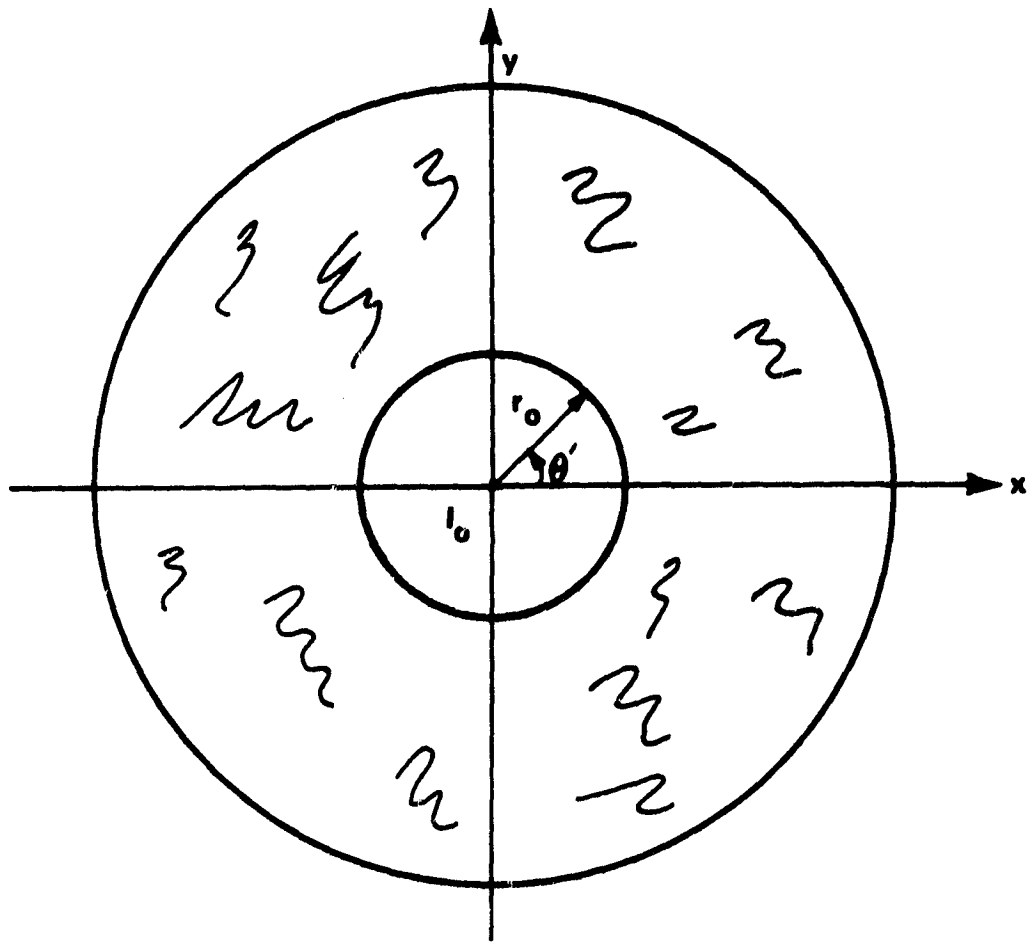

FIGURE 1(a) - INTENSITY DISTRIBUTION OF A CIRCULAR DISC WITH A NOISY BACKGROUND.

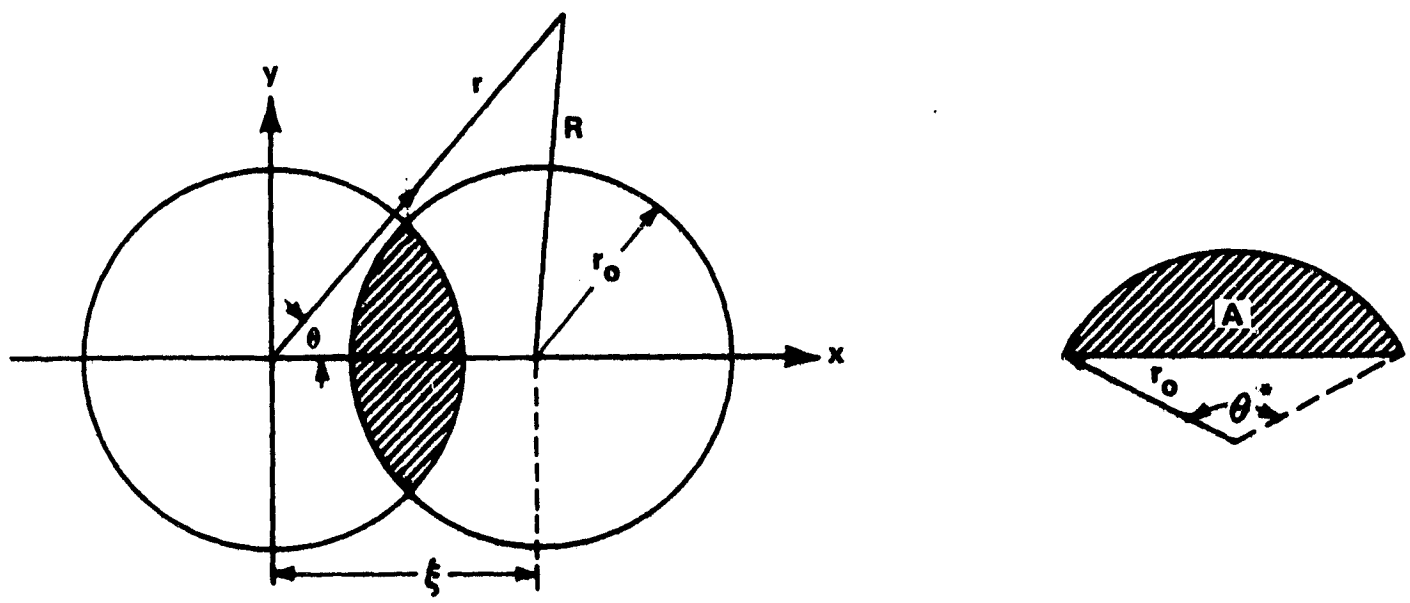

FIGURE 1(b) - CALCULATION OF THE AUTOCORRELATION FUNCTION OF THE SIGNAL DISTRIBUTION FOR A CIRCULAR DISC WITH RADIUS r_o.

As shown in Figure 1(b), equation (8) can be represented by the volume of the intensity times the overlapped area of two discs with radius r_0. First, notice that the area of the shaded region A is

$$\text{Area}(A) = \frac{r_0^2}{2} [\theta^* - \sin \theta^*] \qquad (9)$$

where θ^* is in radians. Secondly, the overlapped area is equal to twice the shaded region A. Thus,

$$\text{Area of Overlapped Discs} = r_0^2[\theta^* - \sin \theta^*] \qquad (10)$$

and the volume is

$$\phi'_{s,s}(\xi) = I_0^2 r_0^2 (\theta^* - \sin \theta^*) \qquad (11)$$

Also from Figure 1(b) or equation 8, we see that θ^* is a function of ξ and their relationship can be expressed as

$$\theta^* = 2 \cos^{-1} \left(\frac{\xi}{2r_0}\right) \qquad (12)$$

By substituting (12) into (11) and noting that

$$\cos^{-1} a = \sin^{-1} \sqrt{1-a^2} \qquad (13)$$

the autocorrelation function of the signal intensity distribution (6) is obtained

$$\phi'_{s,s}(\xi) = 2I_0^2 r_0^2 \left[\cos^{-1}\left(\frac{\xi}{2r_0}\right) - \frac{\xi}{2r_0}\sqrt{1-\left(\frac{\xi}{2r_0}\right)^2}\right] \quad \xi \leq 2r_0 \qquad (14)$$

A plot of (14) is shown in Figure 2. The energy spectrum of this signal pattern can be evaluated by taking the Fourier transform of the autocorrelation function. Before evaluating the Fourier transform we observe the circular symmetry of the autocorrelation function and note that for such a case the two-dimensional Fourier transform reduces to a Hankel transform.[4,5] Thus equations (4) and (7) can now be expressed as

$$\Phi_{s,s}(\omega_x,\omega_y) = \bar{\Phi}_{s,s}(\rho) = 2\pi \int_0^\infty \phi'_{s,s}(\xi) J_0(2\pi\xi\rho)\,\xi\,d\xi \qquad (15)$$

and

$$H_{opt}(\omega_x,\omega_y) = \bar{H}_{opt}(\rho) = \frac{\bar{\Phi}_{s,s}(\rho)}{\bar{\Phi}_{s,s}(\rho)+\bar{\Phi}_{n,n}(\rho)} \qquad (16)$$

respectively, where $\rho^2 = \omega_x^2+\omega_y^2$, $\xi^2=x^2+y^2$ and J_0 is the Bessel function of zero order. Substituting (14) into (15) we obtain

$$\bar{\Phi}_{s,s}(\rho) = 4\pi I_0^2 r_0^2 \int_0^{2r_0} \xi\left[\cos^{-1}\left(\frac{\xi}{2r_0}\right) - \frac{\xi}{2r_0}\sqrt{1-\left(\frac{\xi}{2r_0}\right)^2}\right]$$

$$J_0(2\pi\rho\xi)\,d\xi \qquad (17)$$

It should be noted that the evaluation of (17) is difficult and probably the resulting $\bar{\Phi}_{s,s}(\rho)$ expression will be complicated.

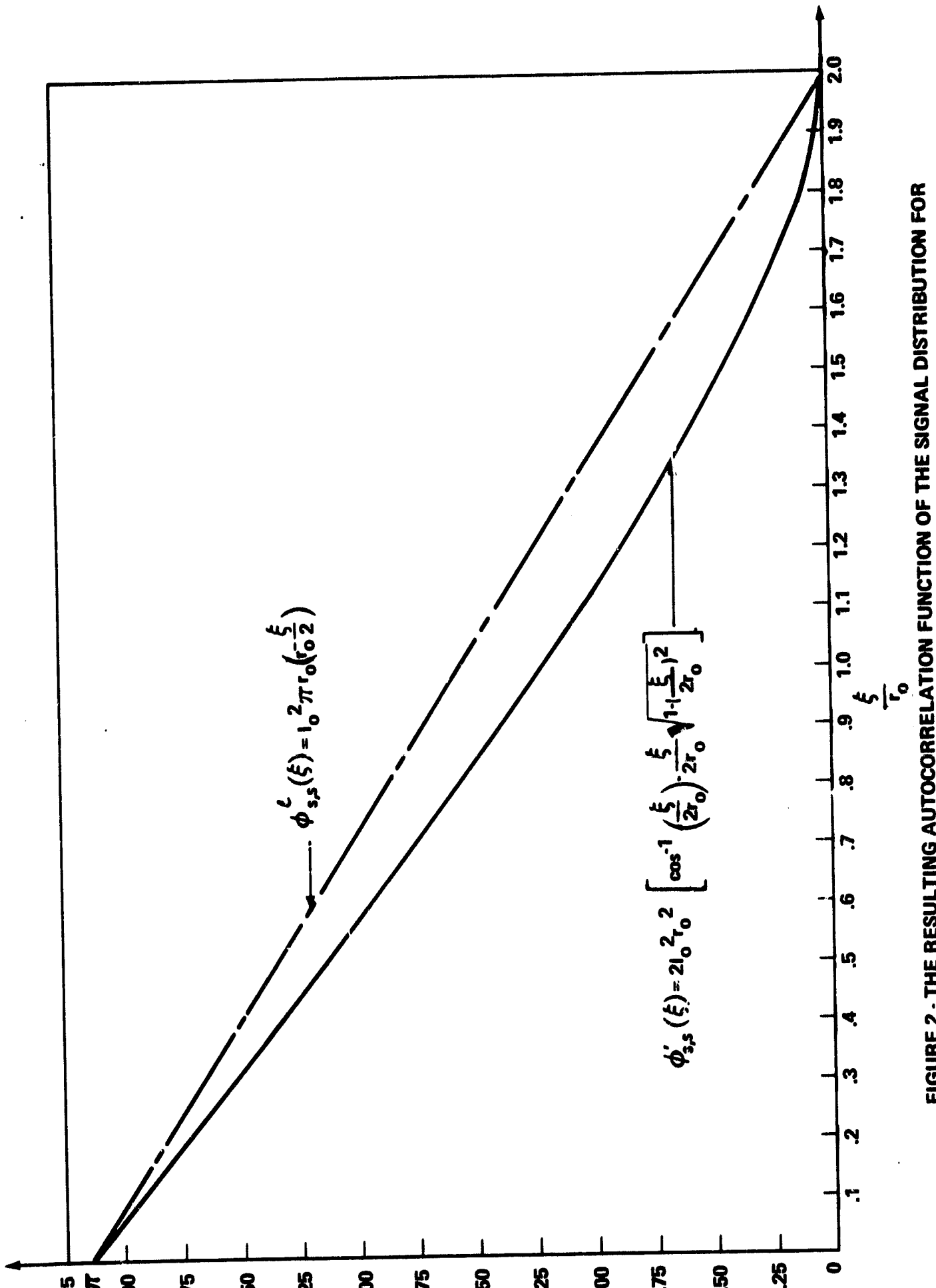

FIGURE 2 - THE RESULTING AUTOCORRELATION FUNCTION OF THE SIGNAL DISTRIBUTION FOR A CIRCULAR DISC WITH RADIUS r_o.

However, by examining the plot of Figure 2, we see that $\phi'_{s,s}(\xi)$ can be closely approximated by a linear equation, which is

$$\phi'_{s,s}(\xi) \cong \phi^{\ell}_{s,s}(\xi) = I_0^2 \pi r_0 (r_0 - \tfrac{\xi}{2})^*, \quad 0 \leq \xi \leq 2r_0$$

Hence (17) can be approximated as

$$\bar{\Phi}_{s,s}(\rho) \cong 2(I_0\pi)^2 r_0 \int_0^{2r_0} (r_0 - \tfrac{\xi}{2})\, J_0(2\pi\rho\xi)\, \xi d\xi \qquad (19)$$

or

$$\bar{\Phi}_{s,s}(\rho) \cong [2(I_0\pi)^2 r_0]\left[\int_0^{2r_0} r_0 \xi J_0(2\pi\rho\xi)\, d\xi - \int_0^{2r_0} \tfrac{\xi^2}{2} J_0(2\pi\rho\xi)\, d\xi\right] \qquad (20)$$

For convenience let

$$I_1 = \int_0^{2r_0} r_0 \xi J_0(2\pi\rho\xi)\, d\xi \qquad (21)$$

and

$$I_2 = \int_0^{2r_0} \tfrac{\xi^2}{2} J_0(2\pi\rho\xi)\, d\xi \qquad (22)$$

---

*Note that this linear equation is chosen because of the initial and final value conditions.

then (20) can be rewritten as

$$\bar{\Phi}_{s,s}(\rho) \cong 2(I_0\pi)^2 r_0 (I_1 - I_2) \tag{23}$$

By letting

$$z = 2\pi\rho\xi \quad \text{and} \quad dz = 2\pi\rho d\xi \tag{24}$$

equation (21) can be transformed as

$$I_1 = \frac{r_0}{(2\pi\rho)^2} \int_0^{4\pi\rho r_0} zJ_0(z)dz \tag{25}$$

The following recurrence relationship holds for all integers n,

$$J_n'(z) = J_{n-1}(z) - \frac{n}{z} J_n(z) \quad . \tag{26}$$

For n=1, it reduces to

$$J_1'(z) = J_0(z) - \frac{J_1(z)}{z} \tag{27}$$

or

$$[zJ_1(z)]' = zJ_0(z) \tag{28}$$

Therefore

$$\int_0^{z_0} rJ_0(r)dr = \left[rJ_1(r)\right]_0^{z_0} = z_0J_1(z_0) \qquad (29)$$

Thus, integral (25) becomes

$$I_1 = \frac{2r_0^2}{(2\pi\rho)} \; J_1(4\pi\rho r_0) \qquad (30)$$

or

$$I_1 = \frac{d^2}{2(2\pi\rho)} \; J_1(2\pi\rho d) \qquad (31)$$

where $d = 2r_0$ is the diameter of the circle.

Integral (22) can be rewritten as

$$I_2 = \frac{1}{2(2\pi\rho)^3} \int_0^{4\pi\rho r_0} z^2 J_0(z)dz \qquad (32)$$

by setting

$$z = 2\pi\rho\xi \quad \text{and} \quad dz = 2\pi\rho d\xi \; . \qquad (33)$$

It has been shown in Reference [6] that

$$\int z^2 J_0(z)\,dz = z^2 J_1(z) + z J_0(z) - \int J_0(z)\,dz \qquad (34)$$

Therefore integral (25) is evaluated as

$$I_2 = \frac{1}{2(2\pi\rho)^3}\left[(4\pi\rho r_0)^2 J_1(4\pi\rho r_0) + (4\pi\rho r_0) J_0(4\pi\rho r_0) - \int_0^{4\pi\rho r_0} J_0(z)\,dz\right] \qquad (35)$$

or

$$I_2 = \frac{1}{2}\left[\frac{d^2}{(2\pi\rho)} J_1(2\pi\rho d) + \frac{d}{(2\pi\rho)^2} J_0(2\pi\rho d) - \frac{1}{(2\pi\rho)^3}\int_0^{2\pi\rho d} J_0(z)\,dz\right] \qquad (36)$$

Hence, substituting (31) and (36) into (23), the autocorrelation energy spectrum of the signal pattern is expressed as

$$\bar{\Phi}_{s,s}(\rho) \cong (I_0\pi)^2 \frac{d}{2}\left[\frac{1}{(2\pi\rho)^3}\int_0^{2\pi\rho d} J_0(z)\,dz - \frac{d}{(2\pi\rho)^2} J_0(2\pi\rho d)\right] \qquad (37)$$

For convenience, let $\omega=2\pi\rho$. Rearranging terms we obtain

$$\bar{\Phi}_{s,s}(\rho) \cong \frac{(I_0\pi d^2)^2}{2}\left[\frac{1}{(\omega d)^3}\int_0^{\omega d} J_0(z)\,dz - \frac{1}{(\omega d)^2} J_0(\omega d)\right] \qquad (38)$$

Since the noise is assumed white and uncorrelated with the signal pattern, its energy spectrum is constant:

$$\bar{\Phi}_{n,n}(\rho) = I_n^2 \tag{39}$$

where I_n is in terms of intensity per (cycles/length) square. Hence, from (16) the required transfer function for an optimal linear filter is

$$\bar{H}_{opt}(\rho) \simeq \frac{q\left[\frac{1}{(\omega d)^3}\int_0^{\omega d} J_0(z)\,dz - \frac{1}{(\omega d)^2} J_0(\omega d)\right]}{1 + q\left[\frac{1}{(\omega d)^3}\int_0^{\omega d} J_0(z)\,dz - \frac{1}{(\omega d)^2} J_0(\omega d)\right]} \tag{40}$$

where $q = 2\pi d^2 (\frac{S}{N})$, and $\frac{S}{N} = \left(\frac{I_0}{I_n}\right)^2 \pi r_0^2$ is defined as signal power to the noise spectral power density. For emphasis it is repeated that the optimum linear filter of (40) is derived by assuming the desired output is a circular disc with uniform intensity. The resolution of a minimal disc was chosen in order to detect objects which can be approximated by a composite of discs of minimal size and larger. This is a two-dimensional analog to the ideal detection of a pulse for the one-dimensional case.

The plot of Figure 3 shows the family of curves of $\bar{H}_{opt}(\omega d)$ for various values of q. The initial value of $\bar{H}_{opt}(\omega d)$, which corresponds to $\omega d=0$, is unity. At the extreme case of $q=\infty$, which corresponds to no noise, $\bar{H}_{opt}(\omega d)=1$. This implies that there is no filter necessary. On the other hand when q is very small or a very large amount of noise present, the optimal $\bar{H}_{opt}(\omega d)$ is

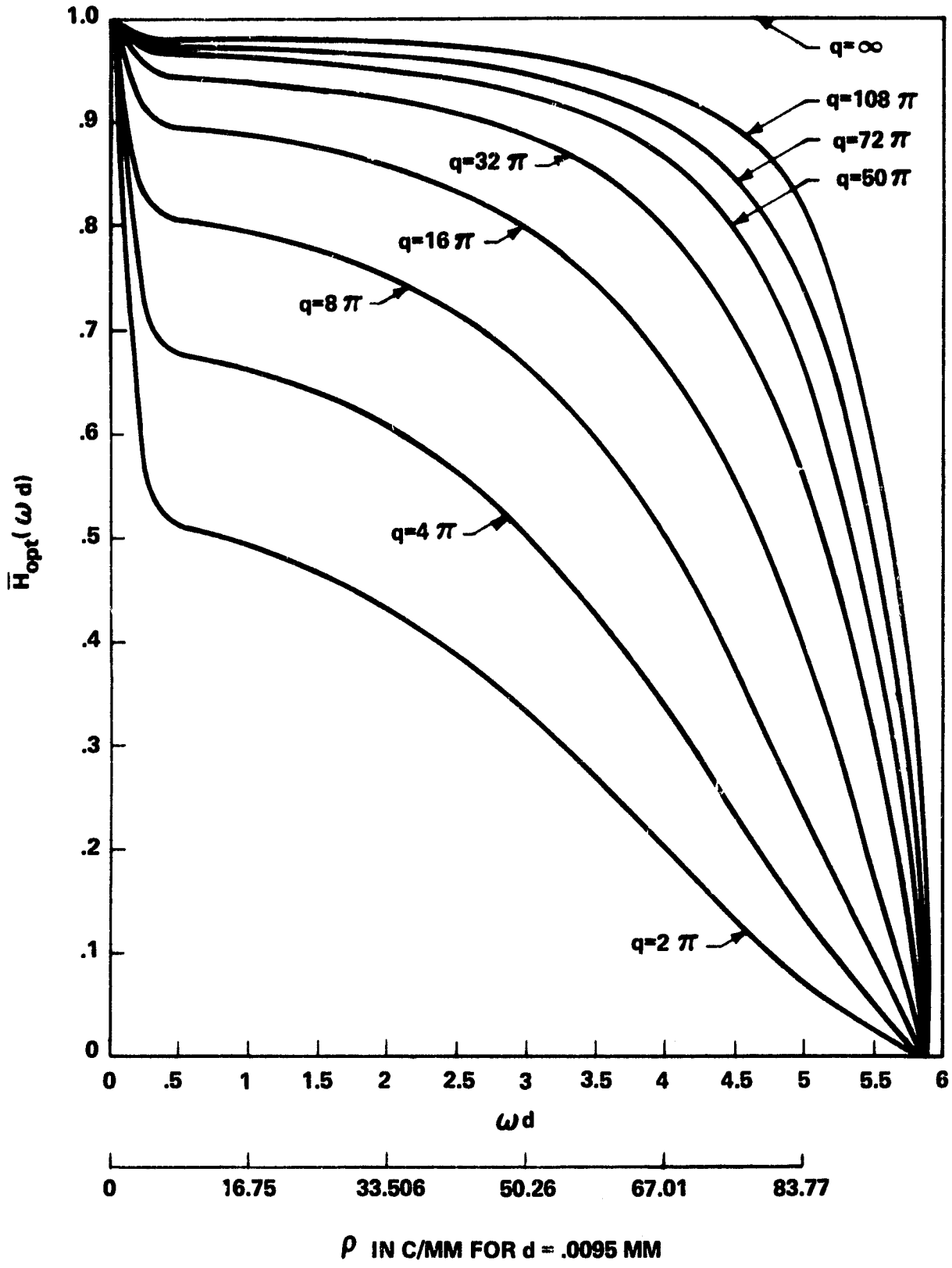

FIGURE 3 - OPTIMUM LINEAR FILTERS DERIVED BY ASSUMING THE DESIRED OUTPUT IS A CIRCULAR DISC WITH UNIFORM INTENSITY.

approximately equal to

$$\overline{H}_{opt}(\omega d) \begin{cases} = 1 \text{ for } \omega d = 0 \\ \simeq q\left[\frac{1}{(\omega d)^3}\int_0^{\omega d} J_0(z)dz - \frac{1}{(\omega d)^2} J_0(\omega d)\right] \end{cases} \quad (72)$$

III. SIMULATION OF THE PHOTOGRAPHIC SYSTEM

The response of the photographic system may be simulated by taking the convolution of the scene array with the inverse transform of the modulation transfer function (MTF). This convolution amounts to taking a two-dimensional weighted average of the point and its neighbors to obtain a value to the corresponding point in the output array. The resolution of the output array can be improved by convoluting it with another array which corresponds to a space filter that compensates for the inadequacies of the MTF and the noise. Figure 4 represents the entire process from scene to improved picture with enhancement and noise filtering; this Figure shows a particular test scene of a white circular disc on a noisy background. The functions beneath the different parts b(x,y), p(x,y), r(x,y) are light intensities at the points (x,y) for the scene, the received photograph and the improved photograph respectively; the functions s(x,y) and f(x,y) are the weights at the points (x,y) of the simulation space filter and the correction filter respectively. Below these functions are their Fourier transforms.

IV. FILTER CONSTRUCTION

From the simulation of Figure 4, the received picture p(x,y) is expressed as

$$p(x,y) = \int_{-\infty}^{\infty}\int_{-\infty}^{\infty} b(x',y')s(x-x',y-y')dx'dy' \quad (42)$$

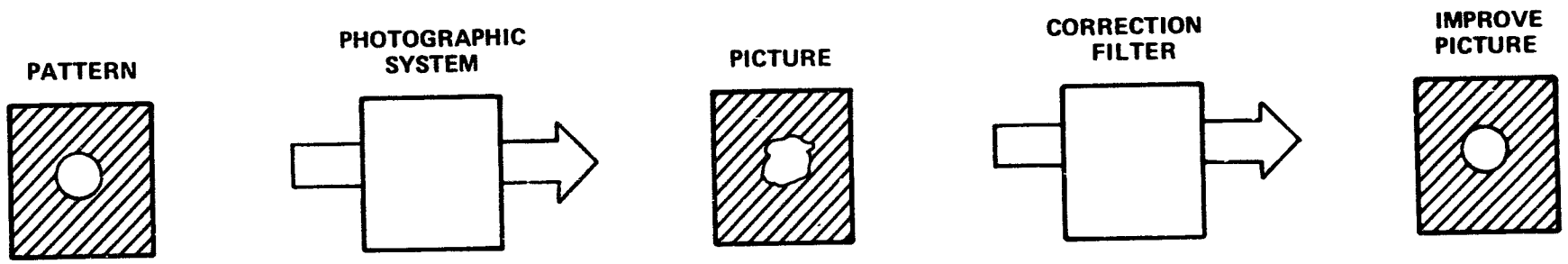

FUNCTION	b(x,y)	s(x,y)	p(x,y)	f(x,y)	r(x,y)
FOURIER TRANSFORMER	$B(\omega_x,\omega_y)$	$S(\omega_x,\omega_y)$	$P(\omega_x,\omega_y)$	$F(\omega_x,\omega_y)$	$R(\omega_x,\omega_y)$

FIGURE 4 - SIMULATION OF THE ENTIRE PROCESS FROM SCENE TO IMPROVE PICTURE WITH ENHANCEMENT AND NOISE FILTERING.

and the corresponding two-dimensional Fourier transform of $p(x,y)$ is

$$P(\omega_x,\omega_y) = B(\omega_x,\omega_y) \cdot S(\omega_x,\omega_y) \text{ , all } \omega_x, \text{ all } \omega_y \qquad (43)$$

Similarly, the following convolution gives the improved picture

$$r(x,y) = \int_{-\infty}^{\infty}\int_{-\infty}^{\infty} p(x',y')f(x-x',y-y')dx'dy' \qquad (44)$$

whose Fourier transform is

$$R(\omega_x,\omega_y) = P(\omega_x,\omega_y) \cdot F(\omega_x,\omega_y) \qquad (45)$$

or

$$R(\omega_x,\omega_y) = B(\omega_x,\omega_y) \cdot S(\omega_x,\omega_y) \cdot F(\omega_x,\omega_y) \qquad (46)$$

In Section II, we obtained the optimal linear filter $\bar{H}_{opt}(\omega d)$ for various q's which is indicative of signal to noise ratios. This filter can be simulated as shown in Figure 5.

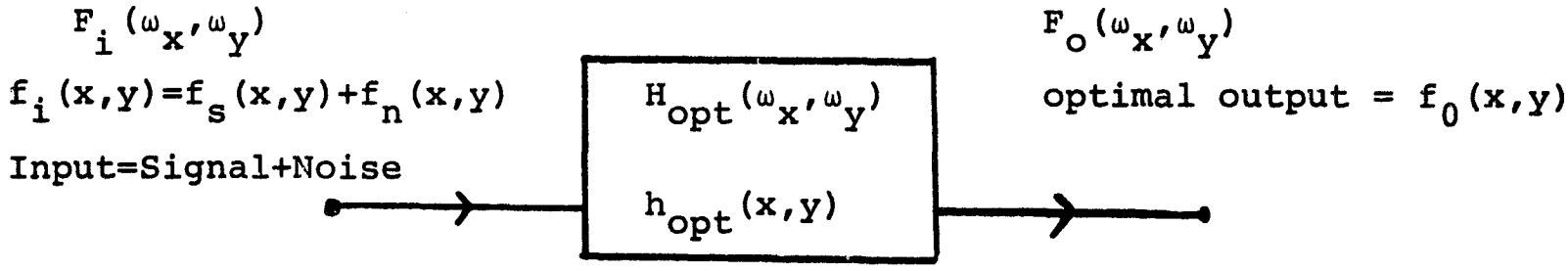

Figure 5 - Simulation of the Optimum Filtering

By comparing the systems of Figures 4 and 5, the following relationships hold

$$F_i(\omega_x,\omega_y) = B(\omega_x,\omega_y) \tag{47}$$

$$F_0(\omega_x,\omega_y) = R(\omega_x,\omega_y) \tag{48}$$

Thus,

$$H_{opt}(\omega_x,\omega_y) = S(\omega_x,\omega_y) \cdot F(\omega_x,\omega_y) \tag{49}$$

or

$$F(\omega_x,\omega_y) = \frac{H_{opt}(\omega_x,\omega_y)}{S(\omega_x,\omega_y)} \quad , \quad \text{all } \omega_x, \quad \text{all } \omega_y \tag{50}$$

$H_{opt}(\omega_x,\omega_y)$ is derived in Section II and $S(\omega_x,\omega_y)$ is generally known[7]; hence, the correction filter $F(\omega_x,\omega_y)$ can be constructed.

In practice, $S(\omega_x,\omega_y)$ is only "known" over a finite region of (ω_x,ω_y); i.e., over the range of frequencies of interest for resolution. Over the remaining portion of (ω_x,ω_y), $S(\omega_x,\omega_y)$ and $H_{opt}(\omega_x,\omega_y)$ are assumed to be constant and therefore integrable in absolute value. The function $F(\omega_x,\omega_y)$ is then designed over the region of interest and as a whole to yield a Fourier transform.

By assuming the modulation transfer function of a lens system to be axially symmetric, its response function is also axially symmetric. Since the modulation transfer function $M(\rho)$, a radial element of the axially symmetric $S(\omega_x,\omega_y)$, is given to characterize the system, it is shown in Reference [4] that $m(r)$, the Hankel transform of $M(\rho)$, is a radial element of the response function $s(x,y)$, i.e., since

$$M(\rho) = S(\omega_x,\omega_y) \tag{51}$$

where $\rho^2 = \omega_x^2 + \omega_y^2$, $M(\rho)$ being in polar coordinates, it follows that

$$m(r) = s(x,y) \tag{52}$$

where $x^2 + y^2 = r^2$, $m(r)$ being the Hankel transform of $M(\rho)$ and in polar coordinates. Thus, from (16) and (51), equation (50) becomes

$$F(\rho) = \frac{\overline{H}_{opt}(\rho)}{M(\rho)} \tag{53}$$

To obtain a practical spatial correction filter, a function $G(\rho)$ (see Figure 6) is defined

$$G(\rho) = \begin{cases} F(\rho) \quad , & \text{for } 0 \leq \rho \leq \Omega \\ \\ \frac{1}{c_0} \quad , & \text{for } \rho > \Omega \end{cases} \tag{54}$$

where Ω ends the region of frequencies of interest and $\frac{1}{c_0}$ is some value which tends to dampen the effect of higher frequency noise; note that c_0 may be picked such that $c_0 = \frac{M(\Omega)}{\overline{H}_{opt}(\Omega)} = \frac{1}{F(\Omega)}$.

Continuing, an auxiliary function $W(\rho)$ (Figure 6) is defined

$$W(\rho) = \frac{1}{c_0} - G(\rho) = \begin{cases} \frac{1}{c_0} - F(\rho) \quad , & \text{for } 0 \leq \rho \leq \Omega \\ \\ 0 \quad , & \text{for } \rho > \Omega \end{cases} \tag{55}$$

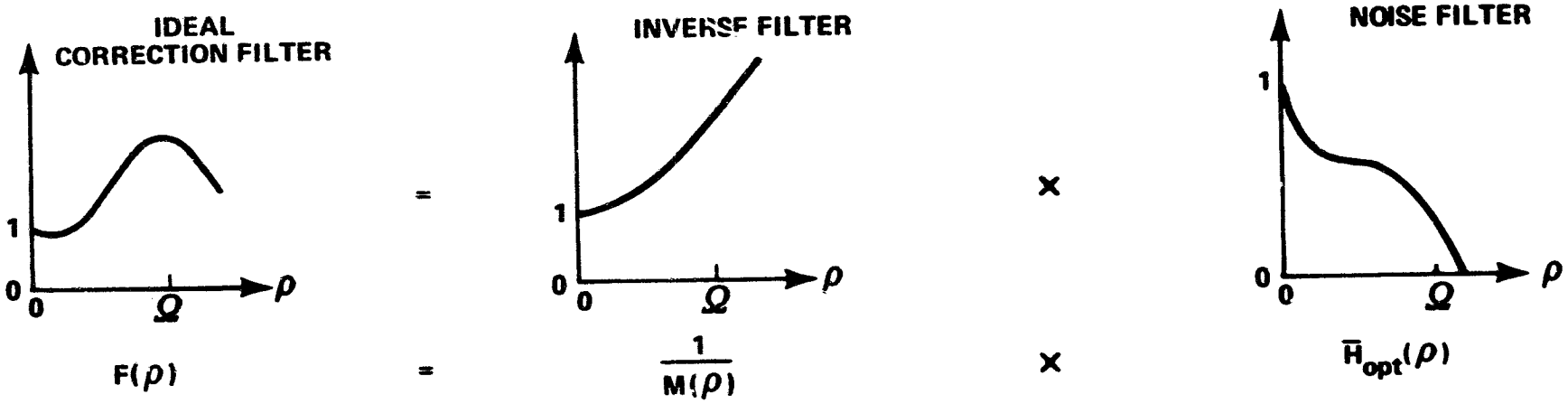

FIGURE 6 - PROCESS FOR OBTAINING A CORRECTION FILTER.

This function also being absolute integrable has a Hankel transform

$$w(r) = 2\pi \int_0^{\infty} W(\rho) J_0(2\pi r\rho) \rho d\rho \tag{56}$$

or since $W(\rho) = 0$ for $\rho > \Omega$

$$w(r) = 2\pi \int_0^{\Omega} W(\rho) J_0(2\pi r\rho) \rho d\rho \tag{57}$$

Hence, the Hankel transform of $G(\rho)$ is

$$g(r) = \frac{1}{c_0} \delta(r) - w(r) \tag{58}$$

where $\delta(r)$ is the Dirac delta function

$$\delta(r) = 0 \text{ for } r \neq 0 \quad \text{and} \quad \int_0^{2\pi} \int_0^{\infty} \delta(r) r dr d\theta = 1 \tag{59}$$

Thus the spatial correction filter to be used in the convolution (44) is

$$f(x,y) = g(r), \quad \text{where } r^2 = x^2 + y^2 \tag{60}$$

V. CORRECTION FILTERS FOR THE LUNAR ORBITER III PICTURES

A computer program has been written to numerically construct a space filter from a spatial frequency function given a cutoff frequency Ω, an error bound e and the resolution limit of the lens system corresponding to minimal size d of a disc recorded on the piece of film. As an illustrative example, four correction filters were constructed from the modulation transfer function of Lunar Orbiter III (Figure 7) with the given input parameters as (Ω=67.5 C/mm, e=.1, $\frac{S}{N} d^2$=4), (Ω=67.5 C/mm, e=.1, $\frac{S}{N} d^2$=8), (Ω=90 C/mm, e=.1, $\frac{S}{N} d^2$=4), and (Ω=90 C/mm, e=.1, $\frac{S}{N} d^2$=8).* The resolution limit of this system corresponding to minimal size of the disc is approximately .0095 mm on the piece of 2.54 mm film, or approximately 3/4 meter on the field size of 200 meter. Thus, by letting d=.0095 mm, the plots of $\bar{H}_{opt}(\rho)$ and $G(\rho)$ for various q's are shown in Figures 3 and 8 respectively. The resulting four correction filters are given in Tables I-IV. The filter values are not axially symmetric since the distance between lines is different than the distance between columns in the picture array.

VI. SUMMARY

Using the two-dimensional Wiener-Hopf equation and assuming the desired output is a circular disc with uniform intensity, optimum linear filters are derived for a given signal to noise ratio. The resolution of a minimal disc was chosen in order to detect objects which can be approximated by a composite of disc of minimal size and larger. This is the two-dimensional analog to the ideal detection of a pulse for the one-dimensional case. As an illustrative example, four spatial correction filters were constructed from the modulation transfer function of Lunar Orbiter III. These filters have been used on a representative picture taken by Lunar Orbiter III. The processed pictures show improvement after filtering is performed.

---

*A method of determining $d^2 \frac{S}{N}$ will be discussed in a later technical memorandum.

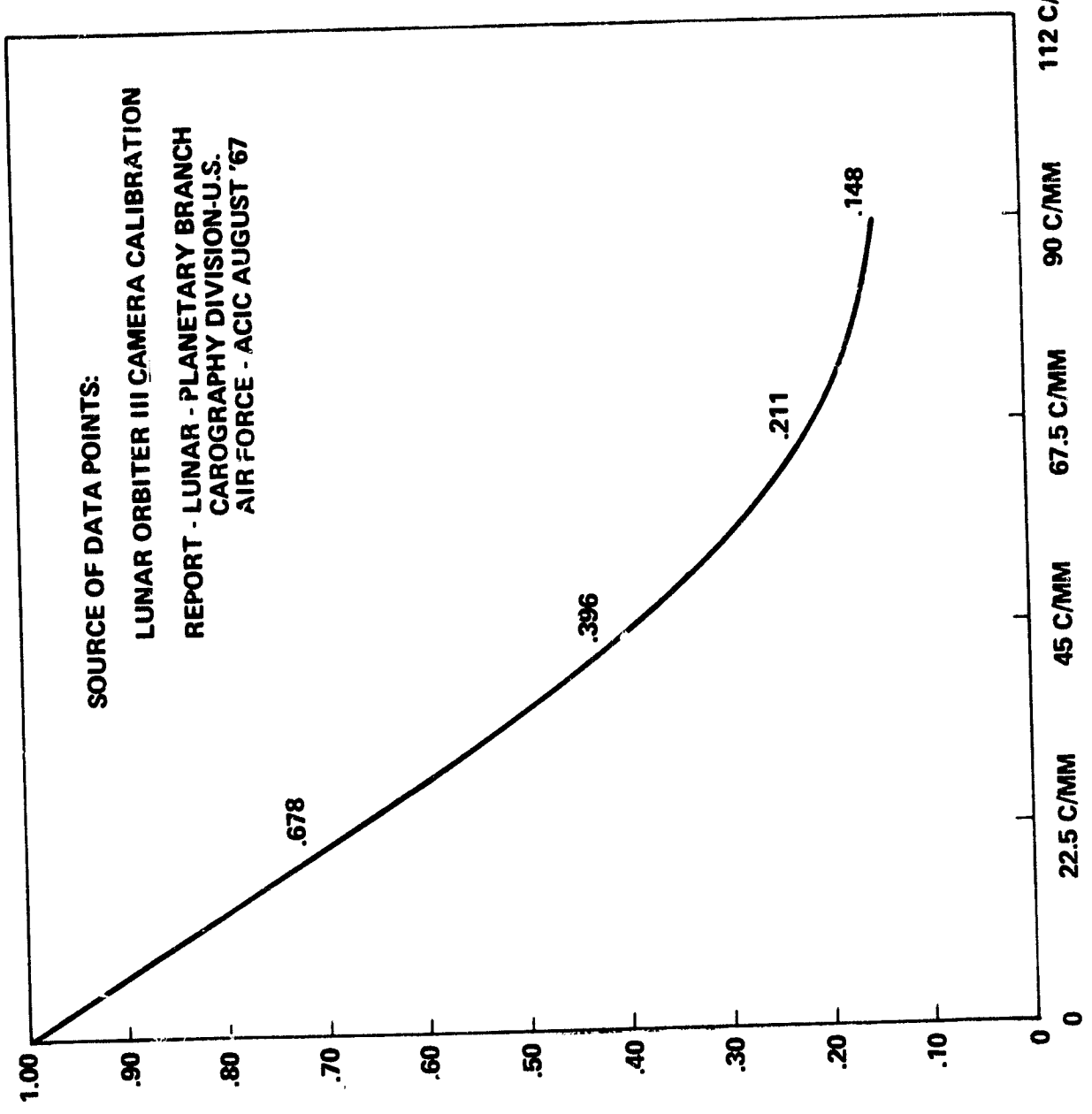

FIGURE 7 - MODULATION TRANSFER FUNCTION OF LUNAR ORBITER III 24-INCH LENS PLUS FILM.

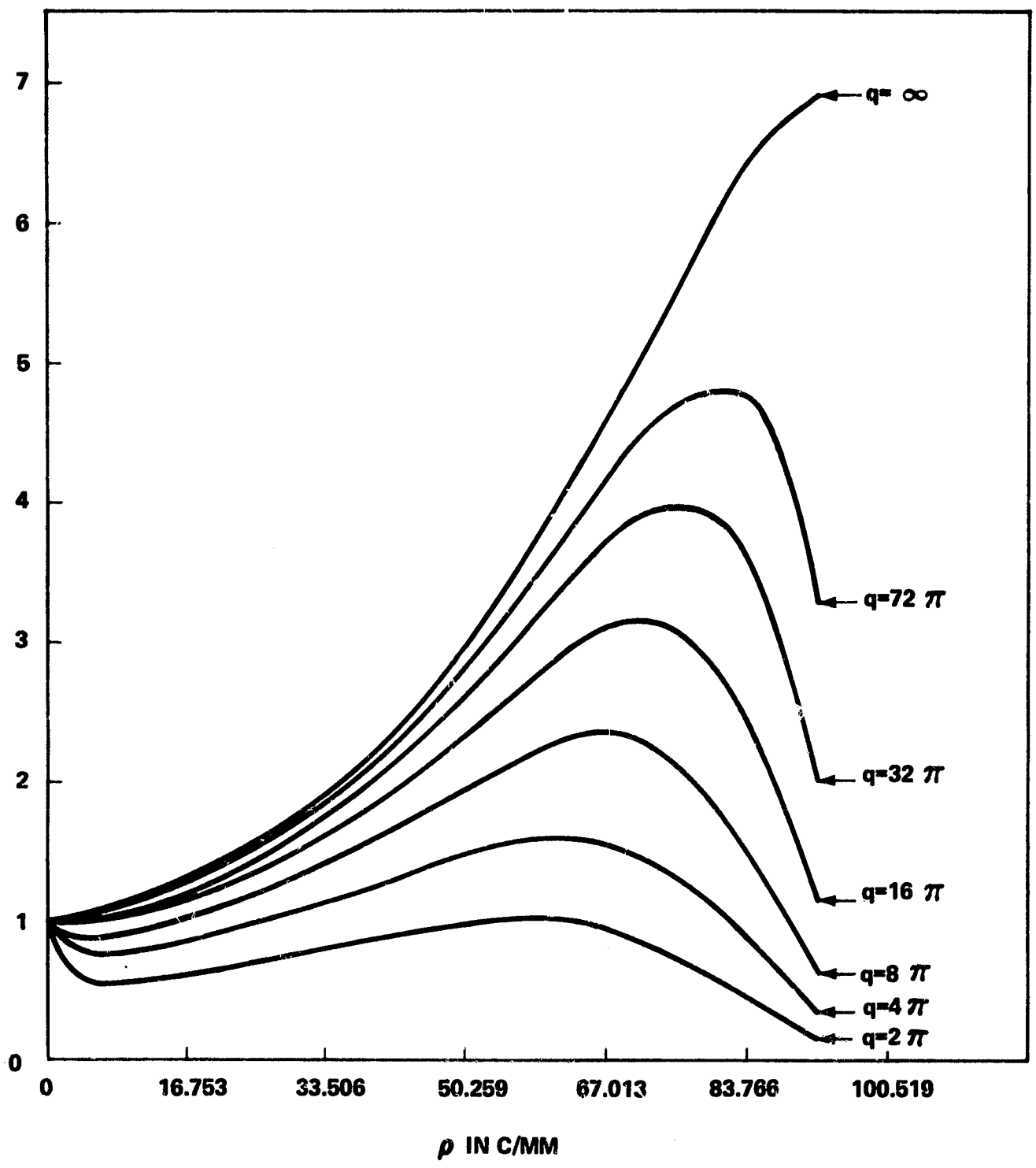

FIGURE 8 - CORRECTION FILTERS FOR LUNAR ORBITER III PICTURES.

i / j	-2	-1	0	1	2
2	-0.01901	-0.04426	-0.05618	-0.04426	-0.01901
1	-0.03638	-0.07380	-0.09099	-0.07380	-0.03638
0	-0.04392	-0.08294	2.24856	-0.08294	-0.04392
-1	-0.03638	-0.07380	-0.09099	-0.07380	-0.03638
-2	-0.01901	-0.04426	-0.05618	-0.04426	-0.01901

TABLE I - CORRECTION FILTER FOR LUNAR ORBITER III PICTURES WITH Ω = 67.5 C/MM; e=0.1 AND $\frac{s}{N} d^2$ =4.

j \ i	-2	-1	0	1	2
2	-0.02289	-0.06650	-0.08804	-0.06650	-0.02289
1	-0.05253	-0.12065	-0.15312	-0.12065	-0.05253
0	-0.06591	-0.14420	2.95281	-0.14420	-0.06591
-1	-0.05253	-0.12065	-0.15312	-0.12065	-0.05253
-2	-0.02289	-0.06650	-0.08804	-0.06650	-0.02289

TABLE II - CORRECTION FILTER FOR LUNAR ORBITER III PICTURES WITH Ω = 67.5 C/MM, e=0.1 AND $\frac{s}{N} d^2 = 8$.

i / j	-2	-1	0	1	2
1	-0.06723	-0.06612	-0.03179	-0.06612	-0.06732
2	-0.07738	0.05475	0.17739	0.05475	-0.07738
0	-0.06678	0.14032	1.18561	0.14032	-0.06678
-1	-0.07738	0.05475	0.17739	0.05475	-0.07738
-2	-0.06723	-0.06612	-0.03179	-0.06612	-0.06723

TABLE III - CORRECTION FILTER FOR LUNAR ORBITER III PICTURES WITH Ω = 90 C/MM, e=0.1 AND $\frac{s}{N} d^2 = 4$.

i / j	2	-1	0	1	2
-2	-0.06828	-0.08843	-0.06274	-0.08843	-0.06828
-1	-0.09333	0.01367	0.12985	0.01367	-0.09333
0	-0.08884	0.09419	1.80057	0.09419	-0.08884
1	-0.09333	0.01367	0.12985	0.01367	-0.09333
2	-0.06828	-0.08843	-0.06274	-0.08843	-0.06828

TABLE IV - CORRECTION FILTER FOR LUNAR ORBITER III PICTURES WITH Ω = 90 C/MM, e= 0.1 AND $\frac{s}{N} d^2 = 8$.

VII. ACKNOWLEDGMENT

Appreciation is hereby expressed to Messrs. H. A. Helm and L. D. Nelson for many fruitful discussions.

S. Y. Lee

1033-SYL-jf

Attachment
References

REFERENCES

1. Elias, P., Grey, D. S. and Robinson, D. Z., "Fourier Treatment of Optical Processes," J. Opt. Soc. Am., vol. 42, (February 1952) pp. 127-134.

2. Robinson, D. Z., "Methods of Background Description and Their Utility," Proceedings of IRE, (September 1959), pp. 1554-1561.

3. Aroyan, G. F., "The Technique of Spatial Filtering," Proceedings of IRE, (September 1959) pp. 1561-1568.

4. Nelson, L. D., "A Digital Filter Method for Improvement of Photographic Resolution," Bellcomm Technical Memorandum, TM-67-1033-3, (August 31, 1967).

5. Bracewell, R., The Fourier Transform and Its Applications, McGraw-Hill, 1965.

6. Lee, S. Y., "A Practical Method for Evaluation of Hankel Transforms," Bellcomm Memorandum for File, July 16, 1968.

7. Lugt, A. V. and Mitchel, R. H., "Technique for Measuring Modulation Transfer Functions of Recording Media," J. Opt. Soc. Am., vol. 57, No. 3, (March 1967).

Bellcomm, Inc.

RECOMMENDATION FOR ANNOUNCEMENT AND DISTRIBUTION OF BELLCOMM REPORT

TO: MA-2/Technical Manager, Systems Engineering Support

FROM: MR. W. STRACK, BELLCOMM, INC.

N70-11661

TITLE OF REPORT Digital Filtering for Optimization of Signals Submerged in Noise

AUTHOR(S) S. Y. Lee

REPORT NO./TYPE TM-69-1033-2 REPORT DATE October 7, 1969

CONTRACT NO. NASW-417 TASK NO. 103-6 SECURITY CLASSIFICATION Unclassified

It is recommended that announcement and distribution of subject report be restricted as follows when released to the NASA Scientific and Technical Information Division:

☐ Restriction Category A - Not to be announced but entered on tape with restriction so that report would only be listed on NASA Searches. Distribution restricted to NASA upon specific request.

☐ Restriction Category B - Announce in Special Announcement Bulletin. Distribution restricted to NASA Headquarters and Centers.

☐ Restriction Category C - Announce in "C-STAR". Distribution restricted to NASA, NASA Contractors, and Government Agencies.

☒ Restriction Category D - Announce in "STAR". Unrestricted distribution.

for W. STRACK 10/16/69 DATE

NASA DETERMINATION

TO: NASA Representative, NASA Scientific and Technical Information Facility

THRU: MR. W. STRACK, BELLCOMM, INC.

FROM: MA-2/Technical Manager, Systems Engineering Support

REF: MA-2 Memorandum dated February 25, 1965, to ATSS, Subject: "Release of Bellcomm, Inc., Reports to Scientific and Technical Information Division."

Pursuant to referenced memorandum, subject report is hereby released with the following restrictions on announcement and distribution:

Restriction Category STAR

T. A. KEEGAN 11/19/69 DATE

TO: NASA Representative, NASA Scientific and Technical Information Facility, 5001 Calvert Rd, College Park, Md., 20740

FROM: MR. W. STRACK, BELLCOMM, INC.

☐ Category A report: The foregoing release is forwarded for entering under Category A.

☑ Category B, C, or D report: Two copies of the subject report have been attached hereto. One additional copy is being forwarded to the FOB 10B Library.

for W. STRACK 11/25/69 DATE

cc: NASA Headquarters Library, FOB 10B
Code: USS-10

BA-185 (9-68)